Lattice gauge action suppressing near-zero modes of H_W

Hidenori Fukaya,[1] Shoji Hashimoto,[2,3] Ken-Ichi Ishikawa,[4] Takashi Kaneko,[2,3] Hideo Matsufuru,[2]
Tetsuya Onogi,[5] and Norikazu Yamada[2,3]

[1]*Theoretical Physics Laboratory, RIKEN, Wako 351-0198, Japan*
[2]*High Energy Accelerator Research Organization (KEK), Tsukuba 305-0801, Japan*
[3]*School of High Energy Accelerator Science, The Graduate University for Advanced Studies (Sokendai), Tsukuba 305-0801, Japan*
[4]*Department of Physics, Hiroshima University, Higashi-Hiroshima 739-8526, Japan*
[5]*Yukawa Institute for Theoretical Physics, Kyoto University, Kyoto 606-8502, Japan*

(Received 18 July 2006; published 3 November 2006)

We propose a lattice action including unphysical Wilson fermions with a negative mass m_0 of the order of the inverse lattice spacing. With this action, the exact zero mode of the Hermitian Wilson-Dirac operator $H_W(m_0)$ cannot appear and near-zero modes are strongly suppressed. By measuring the spectral density $\rho(\lambda_W)$, we find a gap near $\lambda_W = 0$ on the configurations generated with the standard and improved gauge actions. This gap provides a necessary condition for the proof of the exponential locality of the overlap-Dirac operator by Hernandez, Jansen, and Lüscher. Since the number of near-zero modes is small, the numerical cost to calculate the matrix sign function of $H_W(m_0)$ is significantly reduced, and the simulation including dynamical overlap fermions becomes feasible. We also introduce a pair of twisted mass pseudofermions to cancel the unwanted higher mode effects of the Wilson fermions. The gauge coupling renormalization due to the additional fields is then minimized. The topological charge measured through the index of the overlap-Dirac operator is conserved during continuous evolutions of gauge field variables.

DOI: 10.1103/PhysRevD.74.094505 PACS numbers: 11.15.Ha, 11.30.Rd, 12.38.Gc

I. INTRODUCTION

In the construction of the lattice chiral fermions, the conventional Wilson-Dirac operator D_W still plays a crucial role. In the domain-wall fermion [1–3] the lattice Dirac operator is nothing but the Wilson-Dirac operator in four dimensions, but the fermion field has interactions also with its fifth dimensional neighbors. The overlap-Dirac operator [4] D contains a matrix sign function of the Hermitian Wilson-Dirac operator $H_W = \gamma_5 D_W$ as

$$D = \frac{1}{\bar{a}}[1 + \gamma_5 \,\mathrm{sgn}(aH_W)], \qquad \bar{a} \equiv \frac{a}{1+s}. \tag{1}$$

An important difference from the usual Wilson fermion is that the mass term is given with a negative value $m_0 = -(1+s)/a$ of the order of the inverse lattice spacing $1/a$. In the limit of vanishing gauge coupling, the parameter s must be between -1 and 1 in order to obtain the single flavor massless fermion; the sign function is well defined since there is a lower bound in the eigenvalue spectrum of $|H_W|$. In the presence of the gauge interaction, H_W could develop zero or near-zero eigenvalues, which makes the the matrix sign function singular. The near-zero mode does not exist for sufficiently smooth background gauge fields $\{U_\mu(x)\}$ satisfying a condition $||1 - P_{\mu\nu}(x)|| < \epsilon$ for all plaquette variables $P_{\mu\nu}(x)$ with ϵ a small number less than $\sim 1/20.49$ [5]. In the actual numerical simulations, however, $||1 - P_{\mu\nu}(x)||$ is larger by an order of magnitude, and the near-zero modes appear quite frequently.

The origin of the near-zero modes is understood as a local lump of the background gauge field (or so-called the dislocation). An analytic example of such a gauge configuration and its associated exact zero mode is given in [6]. Because such a zero mode is localized in space-time, the number of the near-zero modes increases as the lattice volume V is increased. In other words, the spectral density $\rho(\lambda_W)$ of H_W is nonzero at $\lambda_W = 0$, which is true at any finite value of gauge coupling [7]. The localization property of the near-zero modes has recently been studied extensively [8–10], and it is found that they are exponentially localized unless one enters the Aoki phase, where the flavor-parity symmetry is spontaneously broken [11]. Since the radius of the exponential falloff is of the order of lattice spacing a, the effect of the near-zero modes disappears in the continuum limit, and therefore is a lattice artifact.

The effect of the near-zero modes appears as a small residual breaking of chiral symmetry in the domain-wall formulation [12]. Namely, the four-dimensional fermion mode receives additive mass renormalization m_{res} when the lattice extent in the fifth dimension L_5 is finite [13,14]. The problem is not just that m_{res} is finite, but the suppression is only by $1/L_5$ rather than by $\exp(-cL_5)$ as expected for the extended nonzero modes [10,15]. For the overlap fermion, the residual mass can be made arbitrarily small by projecting out the near-zero mode and treating them exactly when one calculates the matrix sign function. The problem however manifests itself in the locality of the overlap-Dirac operator. The locality is proved only when there exists a gap in the spectral density of H_W near zero [16]. Therefore, the existence of the near-zero mode persisting in the infinite volume limit could potentially spoil

the locality of the overlap-Dirac operator and thus the controlled continuum limit of the overlap fermion. Even if there exists nonzero density of the near-zero modes, the locality may still be maintained [8], provided that the near-zero modes are exponentially localized and its exponential falloff is sufficiently fast. The effect of the near-zero modes becomes irrelevant in the continuum limit, as the localization length scales as the lattice spacing a. In this case the locality of the near-zero modes should always be checked in order to make sure that the Aoki phase is not entered.

In this paper we propose the use of the lattice action with two flavors of extra Wilson fermions with the large negative mass m_0. Since the occurrence of the near-zero modes is suppressed by the fermion determinant, we expect that the spectral density $\rho(\lambda_W)$, as defined in (7), vanishes at $\lambda_W = 0$ and the near-zero modes are strongly suppressed. By suppressing the near-zero modes, the problem of locality of the overlap-Dirac operator is essentially solved. Furthermore, the numerical cost for applying the overlap-Dirac operator is significantly reduced, because the cost for projecting out the low-lying eigenmodes is proportional to the eigenvalue density of H_W. This is especially important when one wants to include the dynamical effect of the overlap fermions in the Monte Carlo simulations.

The idea of adding the extra Wilson fermions is very simple and in fact has been around for several years [17–19], but detailed numerical study has been missing until recently. A preliminary report of this work was included in [20], and a paper by Vranas [21] was submitted very recently, after this work had been essentially completed.

With the action that forbids the occurrence of the zero mode, the global topological charge of the gauge field configuration cannot change through continuous deformation of the gauge variable. This is because the spectral flow of $H_W(m)$ can never cross zero at $m = m_0$ under the continuous deformation. Here we use the index of the overlap-Dirac operator constructed from $H_W(m_0)$ as a definition of the topological charge. Unlike the measurement of the $F\tilde{F}$ operator after some cooling, this always gives an unique integer for the topological charge. The property of conserving topological charge resembles that of the continuum theory. In the continuum theory, there is an infinitely high barrier in the action between different topological sectors, but the barrier is lowered by the lattice regularization of gauge field. With the extra Wilson fermions the infinite potential barrier is recovered at any finite lattice spacing, and thus the continuum gauge field is better approximated.

For the Monte Carlo simulations including the fermion determinant, the Hybrid Monte Carlo (HMC) [22] provides the most efficient algorithm. HMC is based on the molecular dynamics evolution of gauge field variables under the Hamiltonian including a pseudofermion action $\chi^\dagger H_W^{-2}\chi$. The gauge field evolves with small time steps, that approximate the continuous evolution. When a near-zero mode of H_W appears and further approaches the zero point, the pseudofermion action increases rapidly and generates a repulsive force. This means that the topological charge cannot change during the HMC simulation, as far as the step size is taken small enough. If the step size is so large that the transmission through the potential barrier is allowed, the conservation of the Hamiltonian becomes poor and the acceptance rate of the Monte Carlo would become very low.

Since the topological charge does not change, the HMC simulation is confined in an initially given topological sector, and the correct sampling of the $\theta = 0$ (or any finite value of θ) is not possible. This is an advantage for the simulations in the ϵ-regime of the chiral perturbation theory (ChPT) [23], for which one needs the gauge ensemble in a given topological sector. For this purpose, some of the present authors tested a modified plaquette gauge action to suppress the topology change [24] (see also [25]). The proposal of the present work is more solid, as it strictly prohibits the topology change. Out of the ϵ-regime, on the other hand, the fixed topology is a disadvantage. But the possible errors due to the incorrect sampling of the $\theta = 0$ vacuum disappear quickly as the physical volume is increased.

Although we aim at performing dynamical fermion simulations using the overlap formalism, this paper focuses on the quenched study. Namely, the dynamical overlap fermion is switched off, while the extra Wilson fermions are treated dynamically. We then numerically study the spectral density of H_W for various choices of gauge actions.

The rest of this paper is organized as follows. In Sec. II we introduce the lattice actions that we studied in this work. An implementation in the HMC simulation is also presented. Our numerical simulations are explained in Sec. III. Section IV contains the main results of this work, i.e. the spectral density of H_W with and without the extra Wilson fermions. The topology conservation is a key property of the extra Wilson fermions. We discuss how it works (Sec. V) and what is its effect on physical quantities (Sec. VI). In Sec. VII, we calculate how much the gauge coupling is renormalized by the extra Wilson fermions, and show that the finite renormalization can be made small by further adding pseudofermions with a twisted mass term. Section VIII contains our conclusion as well as some discussions about possible artifacts due to the fixed topology.

II. LATTICE ACTION AND ITS IMPLEMENTATION

We consider a lattice action

$$S = S_G + S_E, \tag{2}$$

where S_G is any gauge action, such as the Wilson, Lüscher-Weisz, Iwasaki, etc., and S_E denotes the extra Wilson

fermion. In the following numerical analysis, we use for the gauge part S_G the plaquette gauge action $S_{\rm Pl}$, with and without a modification to suppress dislocations, and the renormalization group (RG) improved (or Iwasaki) action $S_{\rm RG}$. The plaquette action is written as

$$S_{\rm Pl} = \begin{cases} \beta \sum_{x,\mu<\nu} \frac{1-\mathrm{Re\,Tr}P_{\mu\nu}(x)/3}{1-(1-\mathrm{Re\,Tr}P_{\mu\nu}(x)/3)/\epsilon}, & \text{when } 1-\mathrm{Re\,Tr}P_{\mu\nu}(x)/3 < \epsilon, \\ \infty & \text{otherwise} \end{cases}, \tag{3}$$

where $P_{\mu\nu}(x)$ is the plaquette variable at x on the μ-ν plane. The denominator is introduced to suppress the local lump of the gauge field for which $1 - \mathrm{Re\,Tr}P_{\mu\nu}(x)/3$ takes a large value [24–26]. When $1/\epsilon = 0$, it reduces to the standard Wilson gauge action. For this gauge action with a finite $1/\epsilon$, $1 - \mathrm{Re\,Tr}P_{\mu\nu}(x)/3$ cannot become larger than the parameter ϵ. If ϵ is chosen smaller than $1/20.49$, then the Hermitian Wilson-Dirac operator is proved to have a gap [5], but we take a larger number $3/2$ in the numerical simulations, because otherwise the lattice spacing becomes too small even at the strong coupling limit. Another choice of the gauge action is that of Iwasaki [27], which includes the rectangular term with the parameter $c_1 = -0.331$. The denominator as in (3) is not introduced for this case, but it is known that the rectangular term has an effect to suppress the dislocations.

The extra fermion term S_E is written as

$$S_E = \sum_x \bar{\psi}(x) D_W(m_0)\psi(x) + \sum_x \phi^\dagger(x)[D_W(m_0) + i\mu\gamma_5\tau_3]\phi(x), \tag{4}$$

where ψ denotes two flavors of extra heavy Wilson fermion with a negative mass m_0. The second term is a pseudofermion term introduced in order to cancel unwanted effects of the Wilson fermion especially in the ultraviolet region, which leads to a large shift of the β value to be used in the simulation as discussed later in Sec. VII. Because of an additional mass term $\phi^\dagger i\mu\gamma_5\tau_3\phi$, which is twisted in the flavor space by τ_3, the extra Wilson fermion works to suppress the near-zero modes of $H_W(m_0)$ as expected. In fact, the action S_E generates the suppression factor

$$\det\left[\frac{H_W(m_0)^2}{H_W(m_0)^2 + \mu^2}\right] \tag{5}$$

in the partition function. The twisted mass μ controls the range of the near-zero eigenvalues suppressed by the numerator. The eigenvalues whose absolute value is lower than μ are strongly suppressed, while the other higher modes are less affected. The limit of $\mu \to \infty$ corresponds to the case where the pseudofermion term is switched off. When $\mu = 0$, the cancellation is exact, and there is no extra fermions and pseudofermions.

Since the action (2) includes the fermion, some dynamical fermion algorithm is needed to generate the gauge field ensembles. Application of the HMC algorithm is straightforward except for the additional boson term. In order to cancel the higher modes of H_W efficiently, we use only one pseudofermion for both fields. Namely, the Hamiltonian for the molecular dynamics evolution contains a term

$$\sum_x \chi^\dagger(x)\{[D_W(m_0) + i\mu\gamma_5][D_W(m_0)]^{-1}[D_W^\dagger(m_0)]^{-1} \times [D_W^\dagger(m_0) - i\mu\gamma_5]\}\chi(x) \tag{6}$$

with the pseudofermion field χ. Then, the fermion force derived from (6) largely cancels in the combination $[D_W(m_0) + i\mu\gamma_5][D_W(m_0)]^{-1}$, when the twisted mass μ is small.

In the molecular dynamics evolution with (6), an inversion of the Wilson-fermion matrix $D_W^\dagger(m_0)D_W(m_0)$ is necessary, and therefore it costs much more than the usual gauge action. The cost is, however, not substantial compared with the inversion of the overlap-Dirac operator, for instance, needed for the dynamical overlap fermion simulation. The cost for the inversion of H_W^2 is proportional to the inverse of lowest-lying eigenvalue $\lambda_{\rm min}^2$, which is lifted by the introduction of the suppression factor (5). It means that the cost does not increase arbitrarily, even though there is no explicit lower limit on the lowest-lying eigenvalue.

III. HMC SIMULATIONS

We performed Monte Carlo simulations including the extra Wilson fermions. Although the fermions are included, they are unphysical and irrelevant in the continuum limit. The physical sea quarks are not included.

The numerical simulations have been done on a $16^3 \times 32$ lattice with three choices of the gauge actions.

(1) $S_{\rm Pl}$ with $1/\epsilon = 0$, the standard Wilson gauge action.
(2) $S_{\rm Pl}$ with $1/\epsilon = 2/3$. With this choice the plaquette variable $P_{\mu\nu}(x)$ can take any value in the SU(3) gauge group except for the two points $e^{\pm i2\pi/3}I$ with I the 3×3 unit matrix. At these isolated two points, $\mathrm{Re\,Tr}P_{\mu\nu}(x)/3$ becomes minimum. The positivity violation as argued in [28] occurs for ϵ smaller than $3/2$.
(3) $S_{\rm RG}$, the Iwasaki gauge action.

The simulation parameters are listed in Table I. For each of the three choices of the gauge action we take three values of μ, the twisted mass of the extra pseudofermions, to be 0, 0.2, and 0.4. The large negative mass m_0 is always set to -1.6. The gauge coupling β is chosen such that the lattice spacing determined through the Sommer scale

TABLE I. Simulation parameters.

Action	$1/\epsilon$	μ	β	$\delta\tau$	#Trj	$P_{\rm acc}$	$\tau_{\rm int}$	$\langle e^{-\Delta H}\rangle$	r_0/a
Pl	0	0	5.83	0.01	20 000	0.815	21.6	1.005(4)	4.27(29)
Pl	0	0.2	5.70	0.01	11 600	0.812	9.6	0.996(5)	4.08(10)
Pl	0	0.4	5.45	0.01	11 600	0.826	6.4	1.000(6)	3.81(8)
Pl	2/3	0	2.33	0.01	20 000	0.849	3.6	1.002(3)	3.84(5)
Pl	2/3	0.2	2.23	0.01	20 000	0.844	2.1	0.995(3)	3.94(7)
Pl	2/3	0.4	2.06	0.0067	14 800	0.933	2.0	1.000(1)	3.91(11)
RG	···	0	2.43	0.01	20 000	0.781	5.1	0.999(4)	3.91(5)
RG	···	0.2	2.37	0.01	21 600	0.786	4.4	0.998(4)	3.90(7)
RG	···	0.4	2.27	0.01	20 000	0.793	3.5	0.999(4)	3.84(4)

r_0 ($\simeq 0.49$ fm from phenomenological models) is roughly tuned to 0.125 fm, which corresponds to $r_0/a = 3.9$.

All the simulations are carried out using the HMC algorithm, including those with $\mu = 0$, *i.e.* no extra fermions and pseudofermions. The step size $\delta\tau$ of the molecular dynamics evolution with the leapfrog scheme is 0.01 for all lattices except for one choice of the action ($S_{\rm Pl}$ with $1/\epsilon = 2/3$ and $\mu = 0.4$). The unit length of the HMC trajectory is set to 0.5. The total number of the HMC trajectories and observed acceptance rate $P_{\rm acc}$ are listed in Table I. Also listed is the integrated autocorrelation time $\tau_{\rm int}$ measured for the plaquette variable.

It is known that the HMC simulation becomes unstable due to (near-)zero eigenmodes (see, for example, [29]). Since the fermion force F in molecular dynamics steps contains a piece that is proportional to $1/\lambda_{\rm min}$, the step size $\delta\tau$ must be kept small such that the combination $F \times \delta\tau$ is less than $O(1)$. Because there is no explicit lower bound on $\lambda_{\rm min}$ for the Wilson-type fermions, very small eigenvalue could appear, though it is suppressed by the fermion determinant. The problem appears as exceptionally large values of ΔH, the difference of the Hamiltonian between the initial and final steps of the HMC trajectory. In Fig. 1 we show a typical HMC history of ΔH for the lattice "Pl" with $1/\epsilon = 0$ (standard Wilson gauge action). On the left panel we show our main run listed in Table I. ΔH is of order one for most trajectories but develops several large spikes during long runs. We also made a test run with a reduced step size by a factor of 2 ($\delta\tau = 0.005$) and show the result on the right panel, for which the fluctuation of ΔH is reduced and the occurence of the spikes becomes rare.

The volume dependence of the computational cost for the extra Wilson fermion is quite normal. We repeated the test run at $\delta\tau = 0.005$ on a smaller lattice $12^3 \times 24$, and measured the average value of ΔH. With 1000 HMC trajectories we obtain $\langle\Delta H\rangle = 0.0038(23)$, which may be compared with the result on a larger lattice 0.0061(59). Although the statistical error is large, the volume scaling is consistent with the conventional $O(V)$ [30] (or milder), which implies that the total simulation cost scales as $V^{5/4}$. There is no significant spike on both lattice at this small step size.

The exceptional trajectories result in a violation of area preserving property of the leapfrog integration of the molecular dynamics evolution. If it is violated, the detailed

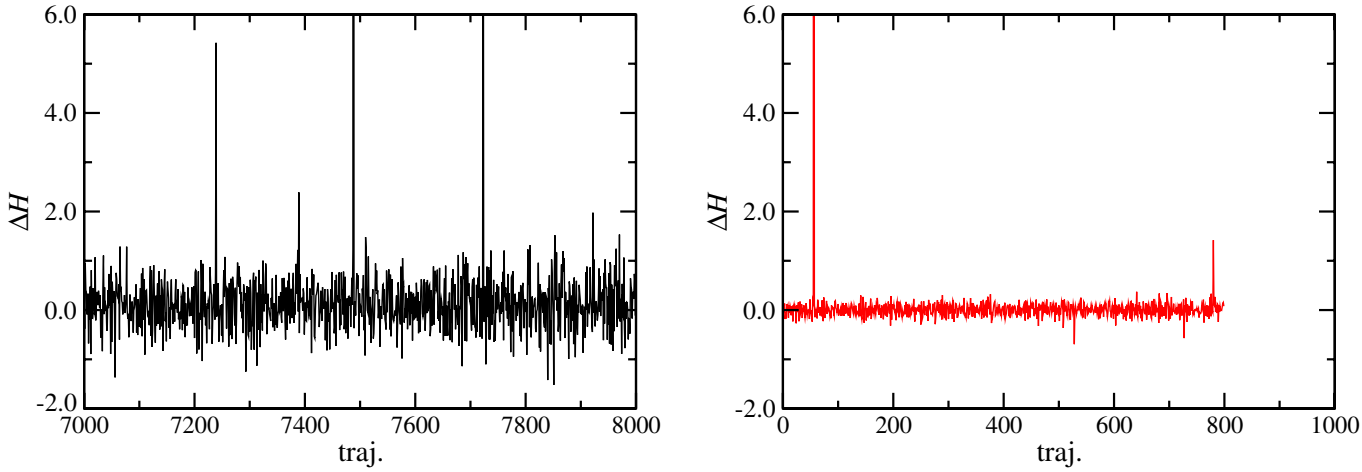

FIG. 1 (color online). History of ΔH for the lattice Pl with $1/\epsilon = 0$. The left panel shows our main run with $\delta\tau = 0.01$, while the right panel is for a reduced step size: $\delta\tau = 0.005$.

balance condition of the Monte Carlo algorithm cannot be proved, and therefore the exactness of the algorithm is lost. This is a problem associated with a discontinuity in the effective pseudofermion action, as in the case for (6). If the step size is small enough, the trajectory would never pass the discontinuity because of the strong repulsive force from the potential wall, and no problem arises. But for some large step size the trajectory may occasionally go across the discontinuity, and then the conservation of the Hamiltonian is strongly violated.

This problem can be monitored by the quantity $\langle e^{-\Delta H}\rangle$, which must be consistent with 1 when the area preserving property is satisfied. In the second last column of Table I we list the value of $\langle e^{-\Delta H}\rangle$. For most cases it is consistent with 1 within 1 standard deviation. The problem is expected to disappear if one chooses small enough step size $\delta\tau$. In fact, for the run Pl with $1/\epsilon = 2/3$ and $\mu = 0.4$, for which $\delta\tau$ is 2/3 of other cases, the number of large spikes is much reduced and the relation $\langle e^{-\Delta H}\rangle = 1$ is satisfied to a good precision.

In the following analysis we assume that the gauge configurations are properly sampled. Even if the exceptional trajectories exist, they are almost always rejected by the Metropolis test and thus do not affect the following trajectories. In the productive run with the dynamical overlap fermion, that we are currently carrying out, the step size is carefully chosen to avoid the potential problem.

IV. SPECTRAL DENSITY

We investigate the effect of the extra Wilson fermions on the spectral density of the Hermitian Wilson-Dirac operator $H_W(m_0)$ in the quenched approximation.

We take 30–100 gauge configurations for each runs listed in Table I and calculate the low-lying eigenvalues of $H_W(m_0)$ with $m_0 = -1.6$. For each runs the gauge coupling is chosen such that the lattice spacing is roughly tuned to 0.125 fm. Statistical correlation between consecutive gauge configurations is negligible, as they are separated by 200 HMC trajectories. We use the conventional Lanczos algorithm, and calculate the eigenvalues with its absolute value less than 0.2 in the lattice unit.

In Fig. 2 we plot the absolute value of the observed eigenvalues λ_W for each set of configurations. Different choices of lattice actions are shown in separate panels, and in each panel the results at three values of μ (0.0, 0.2, and 0.4) are plotted. As one can clearly see, there are significant number of eigenvalues $|\lambda_W|$ less than 0.01 for any of the three gauge actions if the extra Wilson fermions are not included ($\mu = 0$). On the other hand, with the finite values of μ, the eigenvalues less than 0.02 do not appear at all. The difference between $\mu = 0.2$ and 0.4 is not significant, but $\mu = 0.2$ seems slightly better.

These observations can be made more quantitative using the spectral density $\rho(\lambda_W)$. The spectral density is defined by

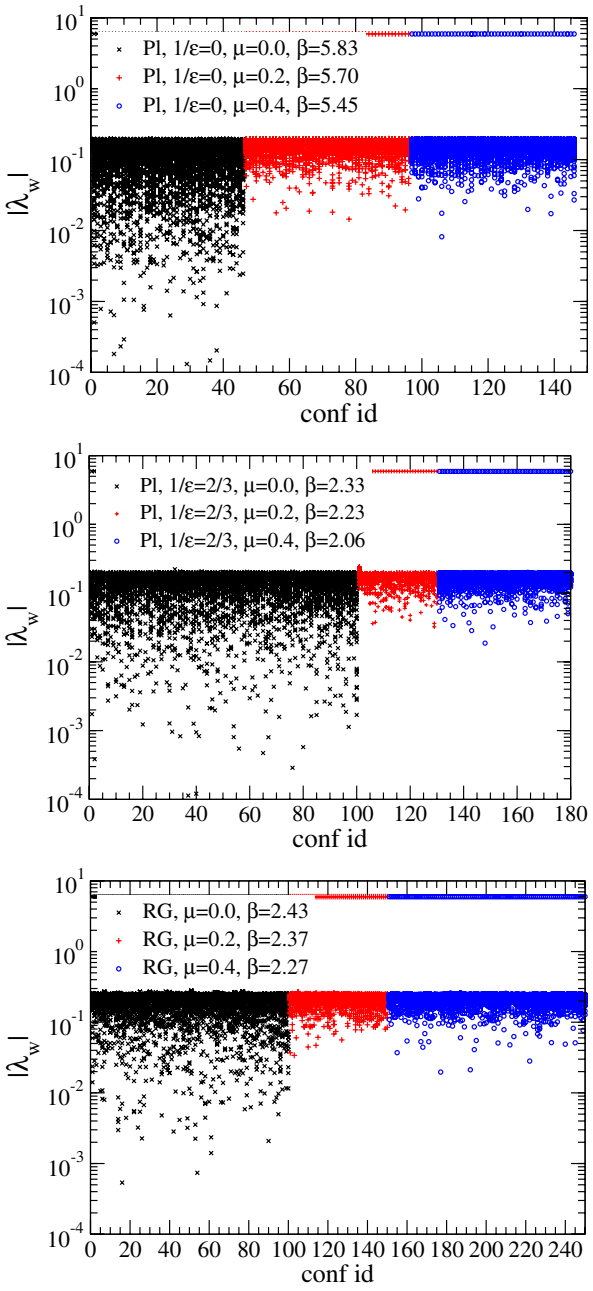

FIG. 2 (color online). Low-lying eigenvalues of $H_W(m_0)$. Lattice actions are Pl with $1/\epsilon = 0$ (top), Pl with $1/\epsilon = 2/3$ (middle), and RG (bottom). Data for three values of μ ($\mu = 0.0$, 0.2, and 0.4) are shown in each plot. The highest mode is also shown, whose value is ~5.9, almost independent of the gauge configuration.

$$\rho(\lambda_W) = \frac{1}{V}\left\langle \sum_n \delta(\lambda_W - \lambda_n)\right\rangle, \tag{7}$$

where $\langle\cdots\rangle$ denotes the ensemble average and λ_n represents each eigenvalue on a given gauge configuration. In Fig. 3 we plot the histogram of $\rho(\lambda_W)$. Each bin in the plots has a size of 0.0192 in λ_W. We observe nonzero spectral density at $\lambda_W = 0$ when there is no extra fermion intro-

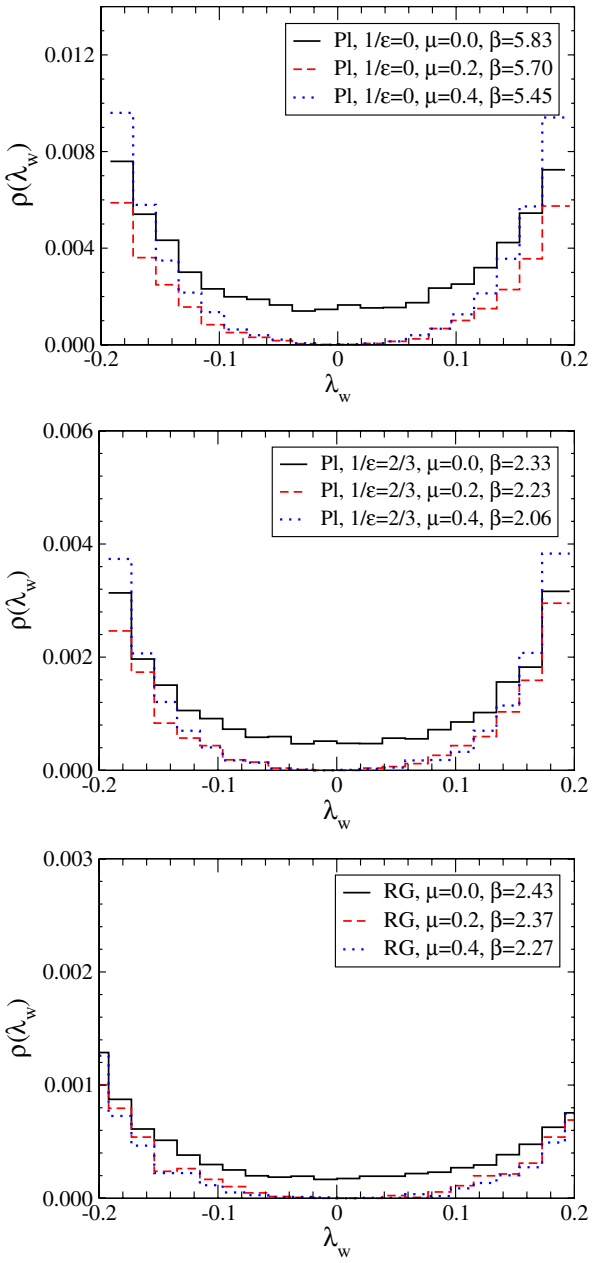

FIG. 3 (color online). Histogram of the spectral density of $H_W(m_0)$. Lattice actions are Pl with $1/\epsilon = 0$ (top), Pl with $1/\epsilon = 2/3$ (middle), and RG (bottom). Data for three values of μ ($\mu = 0.0$, 0.2, and 0.4) are shown in each plot.

duced ($\mu = 0.0$). We calculate the value of $\rho(0)$ by fitting an integrated density $I(\bar{\lambda}) = \int_{-\bar{\lambda}}^{+\bar{\lambda}} d\lambda \rho(\lambda)$ with a polynomial $2\rho(0)\bar{\lambda} + O(\bar{\lambda}^3)$. The results are $\rho(0) = 1.509(3) \times 10^{-3}$ for Pl with $1/\epsilon = 0$, $0.494(1) \times 10^{-3}$ for Pl with $1/\epsilon = 2/3$, and $0.177(1) \times 10^{-3}$ for "RG." As well known, the density of the near-zero modes is substantially reduced for the improved actions.

With the extra Wilson fermions the near-zero mode density is essentially zero; there is no events in the lowest bin. The curve of $\rho(\lambda_W)$ near $\lambda_W = 0$ is consistent with $\sim \lambda_W^2$ for both $\mu = 0.2$ and 0.4. The difference between $\mu = 0.2$ and 0.4 is not significant, except for the highest bin at $|\lambda_W| \simeq 0.2$.

Among the three choices of the gauge actions, the suppression of the near-zero modes is most efficient for the RG action. We should note that the scale of the vertical axis in Fig. 3 is different among the three plots, and the value at $|\lambda_W| \simeq 0.2$ is 6–10 times smaller for the RG action than the standard Wilson gauge action ($1/\epsilon = 0$). The choice Pl with $1/\epsilon = 2/3$ is in between the other two. Therefore, we may conclude that the rectangular term is more effective to suppress the dislocation than restricting the range of the plaquette variable by the denominator in (3).

V. TOPOLOGY CONSERVATION

As we discussed in the introduction, the net topological charge defined as an index of the overlap-Dirac operator cannot change by the continuous deformation of the gauge field variables when the extra Wilson fermion is included. This is approximately the case in our simulation using the HMC algorithm with small molecular dynamics time step $\delta\tau$. The large spikes in ΔH as discussed in Sec. III may indicate some attempts of the gauge field to go beyond the potential barrier, but the acceptance probability of such trajectories is essentially zero and therefore the topology does not change in the accepted trajectories.

In order to explicitly check the topological charge of the generated gauge configurations, we calculate the near-zero eigenmodes of the overlap-Dirac operator D as defined in (1). The kernel operator is the Wilson-Dirac operator with $m_0 = -1.6$, the same value as in the extra Wilson fermion. The topological charge can be identified as the number of the left-handed or right-handed zero modes. In practice we adopt the method proposed in [31]. Namely, we calculate the low-lying eigenvalues of chirally projected operators $D^{\pm} \equiv P_{\pm} D P_{\pm}$. Since the nonzero eigenvalues appear in pair between D^+ and D^-, the remaining unpaired eigenvalues very close to zero can be identified as chiral zero modes.

We calculate the eigenvalues of D on 80 configurations of "RG" with $\mu = 0.2$, and find no exact chiral zero mode. This is consistent with our expectation, as these configurations are generated starting from an initial configuration in the trivial topological sector, i.e. $Q = 0$. In addition, we also generated another set of configurations starting from a $Q = -2$ configuration (number of samples is 60). On all of these configurations we confirm the presence of two left-handed zero modes as expected. From these observations we conclude that the topological charge is indeed conserved during the HMC simulations. We are currently performing many set of simulations including dynamical overlap fermions as well as the extra Wilson fermions. Also in these simulations, there has been no sign of the change of the topological charge so far.

VI. TOPOLOGY DEPENDENCE

Since the topological charge conserves during the HMC simulation, one cannot sample the correct $\theta = 0$ vacuum, for which the topological charge distributes according to the topological susceptibility. However, the cluster decomposition property of the local field theory suggests that the physical quantities measured in a local space-time region do not depend on the topological fluctuations occuring far apart from that region. This means that the physical quantities do not depend on the global topological charge, as far as the space-time volume is large enough. The topological fluctuation is controlled by the topological susceptibility $\chi_t \equiv \langle Q^2 \rangle / V$, which is proportional to $m\Sigma = M_\pi^2 F_\pi^2$ in unquenched QCD near the chiral limit. The typical length scale for the topological fluctuation is then given by $(M_\pi F_\pi)^{-1/2}$. The lightest possible pion mass in our planned dynamical simulation is $M_\pi \simeq 300$ MeV, for which the typical scale is ~ 1 fm. It becomes even smaller for heavier sea quark masses or for the quenched theory. Therefore, our naive expectation is that the fixed-topology simulations in a $(2\ \mathrm{fm})^4$ box or larger do not have too much impact on physical quantities.

On a rather general ground, one can prove that the hadron masses in a fixed topological sector deviate from the correct value in the $\theta = 0$ vacuum by $O(1/\langle Q^2 \rangle)$, which scales as $\sim 1/V$ [32]. An estimate of the coefficient using the chiral effective lagrangian implies that the deviation of pion mass does not exceed 1% even for light pions (~ 300 MeV) on a $(2\ \mathrm{fm})^4$ box, and the effects on other hadrons are even smaller.

In this paper we show a study in the quenched approximation, instead of the time-consuming dynamical fermion simulations. In the quenched theory, however, the situation could be drastically different because the hadron masses are more infrared sensitive due to the double pion pole structure at the one-loop level of quenched chiral perturbation theory. Because of the integral of the form $\int d^4p m_0^2/(p^2 + m_\pi^2)^2$, the diagram is infrared divergent in the chiral limit, and the information of the topological fluctuation of the whole space-time is gathered through the singlet vertex m_0^2 proportional to the topological susceptibility χ_t, whose integral over space-time gives Q^2 the fixed topological charge in this case. We therefore expect the quenched chiral logarithm that depends on the topological charge as Q^2/V rather than its average $\langle Q^2 \rangle / V$.

In order to see the Q dependence in the simulations, we carry out a calculation of pion mass on quenched gauge configurations with fixed topological charges $|Q| = 0, 2, 3,$ and 6. The gauge configurations are generated with the extra Wilson fermions at $\beta = 2.37$ (RG gauge action), and the statistics is 100 for each topological charge. The results for $(am_{PS})^2/(am)$ are plotted in Fig. 4 as a function of the quark mass am. We find rather large topological charge dependence as expected in the quenched theory: the difference of am_{PS} between $|Q| = 0$ and 6 is as large as 10%. A similar dependence is also found in [33].

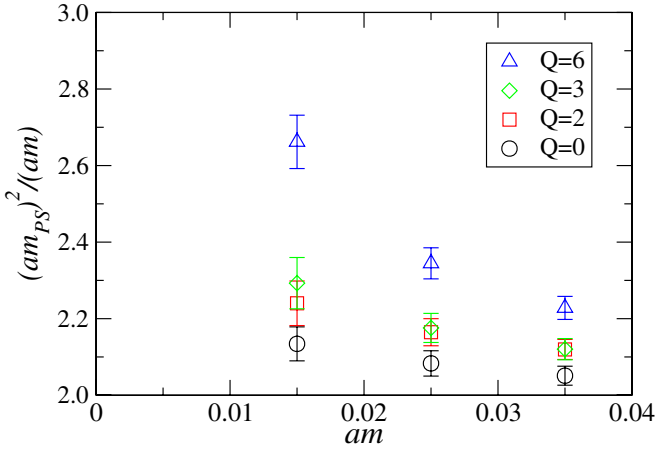

FIG. 4 (color online). Pseudoscalar mass squared calculated on the quenched configurations at fixed topological charges $|Q| = 0$, 2, 3, and 6.

Such a large topology dependence is not expected for unquenched QCD, because there is no pathological infrared divergence. In our on-going dynamical overlap fermion project, we are planning to investigate the topology dependence in detail as well as the volume dependence.

VII. BETA SHIFT

The extra Wilson fermions and their associated pseudofermions have masses of order of the lattice cutoff and do not affect the physics at low energy. Their only effects are ultraviolet ones, such as the renormalization of the strong coupling constant and quark masses. Here we calculate the finite renormalization of the strong coupling constant (or the β shift) due to the extra fields at the one-loop level in perturbation theory. Such calculation for the massless Wilson fermion was done before [34,35], but we must repeat the calculation with the large negative mass.

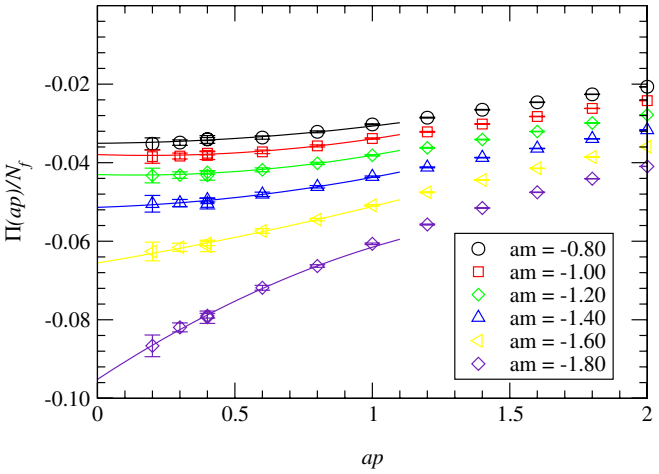

FIG. 5 (color online). $\Pi(p)/N_f$ for various mass parameters.

TABLE II. Vacuum polarization function $\Pi(p)/N_f$ at $p = 0$.

am_0	Without pseudofermion	$\mu = 0.1$	$\mu = 0.2$	$\mu = 0.3$	$\mu = 0.4$
−0.8	−0.0351(2)				
−1.0	−0.0379(2)	−0.000 395(3)	−0.001 53(1)	−0.003 29(3)	−0.005 49(5)
−1.2	−0.0430(3)		−0.001 71(1)		
−1.4	−0.0514(3)		−0.002 28(2)		
−1.6	−0.0655(3)	−0.001 12(1)	−0.004 18(3)	−0.008 44(7)	−0.0133(1)
−1.8	−0.0952(4)		−0.012 09(4)		

The shift of the coupling constant is given as

$$\frac{1}{g_{\rm eff}^{(N_f)2}} = \frac{1}{g_0^2} - \Pi(p), \tag{8}$$

where $\Pi(p)$ is the vacuum polarization function of gluon due to fermions:

$$\Pi_\mu(p) = (p^2\delta_{\mu\nu} - p_\mu p_\nu)\Pi(p). \tag{9}$$

For the usual (lattice) fermions, it is written as

$$\Pi(p) = N_f\left[\frac{1}{24\pi^2}\ln(a^2p^2) + k_f\right], \tag{10}$$

and the constant k_f depends on the fermion formulations. One-loop calculation gives −0.013732 (Wilson fermion) [36,37], −0.038 529 (clover fermion) [38]. The logarithmic term in (10) corresponds to the usual one-loop running of the coupling constant and gives the N_f dependent coefficient of the beta function $b_0 = \frac{1}{(4\pi)^2}(\frac{11}{3}N - \frac{2}{3}N_f)$.

The unphysical fermions with a large negative mass do not contribute to the logarithmic term in (10). Therefore, the $p \to 0$ limit is finite. Figure 5 shows $\Pi(p)/N_f$ for the negative mass Wilson fermion with masses $am = -0.80 \sim -1.80$. Since the numerical integral becomes unstable near $ap = 0$, we obtain the $ap \to 0$ limit by an extrapolation using the data points below $ap = 1$. The numerical results for $\Pi(0)$ are listed in Table II.

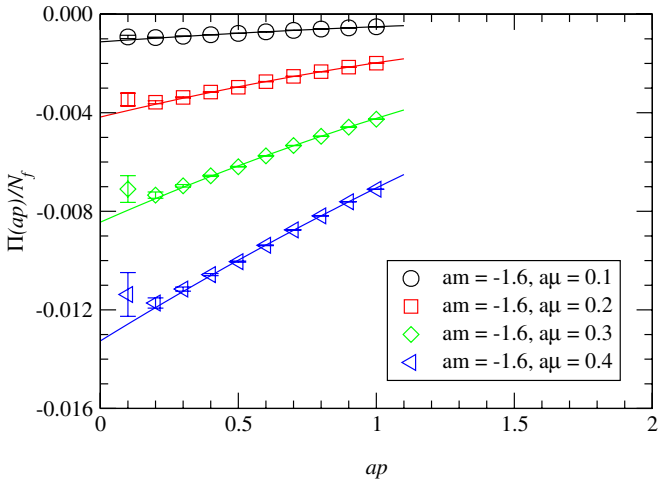

FIG. 6 (color online). $\Pi(p)/N_f$ including the twisted mass pseudofermions.

At $am_0 = -1.6$ the β shift $\delta\beta = -6\Pi(0)$ is calculated as 0.786(4) at the one-loop level. It means that we have to reduce the β value by this amount in order to simulate without changing the lattice spacing. The actual value could be significantly larger due to higher order corrections. With the mean field improvement, for instance, the value is divided by the expectation value of the plaquette $\langle P\rangle$, which is typically around 0.6 for the Wilson gauge action at $\beta = 6$.

Including the twisted mass pseudofermions, the β shift is substantially reduced. It vanishes in the limit of $\mu \to 0$ and the contribution for finite μ starts from μ^2. Results are shown in Fig. 6 for $am_0 = -1.6$ and the twisted mass $\mu = 0.1$–0.4. Note that the vertical axis is 1 order of magnitude smaller than that in Fig. 5. At $\mu = 0.2$, the β shift is 0.0502(4) ($N_f = 2$), which may be compared with the actual data: $\beta = 5.83 \to 5.70$ for Pl with $1/\epsilon = 0$, $2.33 \to 2.23$ for Pl with $1/\epsilon = 2/3$, and $2.43 \to 2.37$ for "RG." The one-loop calculation underestimates the measured value by about a factor of 2 for the plaquette gauge action, while it gives a good approximation for the RG action. This is consistent with the expected mean field enhancement of the coupling constant for the plaquette gauge action.

The small β shift for the cases with the twisted mass pseudofermions is desirable, because one can avoid too small β values in the dynamical fermion simulations. In particular, for the Wilson gauge action there is a remnant of the fundamental-adjoint phase transition [39] in the strong coupling regime ($\beta \lesssim 5.2$). With dynamical fermions it may appear as a real first-order phase transition, which prevents one from taking smooth continuum limit. Examples are found in the simulations with two [40,41] and three flavors [42] of the Wilson-type fermions.

VII. CONCLUDING REMARKS

By introducing the extra Wilson fermions with the large negative mass, it is possible to provide a gap in the spectral density of H_W and thus to remove the problem associated with the near-zero modes. For the overlap fermion the exponential localization of the Dirac operator is guaranteed; for the domain-wall fermion the residual chiral symmetry breaking will be much reduced. For three choices of

gauge actions, we confirm that the spectral density of H_W vanishes at $\lambda_W = 0$ and the occurrence of the near-zero mode is very much suppressed. The number of remaining near-zero modes is smallest for the Iwasaki gauge action. By also adding the twisted mass pseudofermions, the effect on the coupling renormalization can be minimized while keeping the good property of suppressing the near-zero modes.

A remaining problem concerning the locality of the overlap-Dirac operator is its actual localization length in the numerical simulations. For the numerical simulation with controlled discretization error, the localization length has to be much smaller than $1/\Lambda_{\rm QCD}$, and this gives a stronger practical upper limit of the gauge coupling in addition to the more fundamental limit from locality. Golterman, Shamir, and Svetitsky argued that the localization length is controled by the mobility edge of the eigenmodes of H_W [8–10]. We are currently calculating the spatial correlation on the low-lying mode eigenvectors in order to determine the mobility edge. This work will be published elsewhere.

Although the extra Wilson fermion is also useful in the quenched QCD simulations, our main objective is to perform the unquenched simulations using the fermion formulation with exact chiral symmetry. So far, the dynamical overlap fermion simulation has been attempted only on small lattices [43–46], as its computational cost is extremely large. One of the reasons for the large numerical cost is the treatment of the sign function. When the low-lying eigenvalue H_W passes zero during the molecular dynamics evolutions, the sign function changes its value discontinuously and its derivative diverges. Fodor, Katz, and Szabo [43] introduced so-called the reflection/refraction process on the $\lambda_W = 0$ surface, which requires monitoring of the low-lying eigenvalues and takes lots of computational costs. The cost would scale as V^2, as the lattice volume V is increased, and therefore the simulation on large lattices could be prohibitively costly. This problem can be totally avoided by the extra Wilson fermion, because the zero crossing never happens if the molecular dynamics step size is chosen small enough. The extra cost for the Wilson fermion is negligible in the dynamical overlap fermion simulation. Using this lattice action, we are currently carrying out the dynamical overlap fermion simulations on a $16^3 \times 32$ lattice.

An immediate question on the strategy of suppressing the low-lying modes of H_W is that the simulation is trapped in a given topological sector and one cannot achieve the correct sampling of the $\theta = 0$ vacuum of QCD. This is an algorithmic problem of the molecular dynamics simulation, in which the gauge variables are changed continuously along trajectories. We first emphasize that the continuum theory has the same property, *i.e.* the topological nature of the gauge field on a torus. Any lattice gauge action should recover this topological property as the continuum limit is approached, and our choice has this property at any finite lattice spacing. The configuration space of a given fixed topology is simply connected in the continuum limit, and therefore the ergodicity of the Monte Carlo simulation is satisfied even with a fixed topology. At finite lattice spacings there is no proof of the ergodicity, but there is no indication of its violation either. In order to detect such an effect if any, we should probably look at quantities sensitive to the topological charge density. That is an interesting subject, which we leave for future studies.

Second, because of the cluster decomposition principle any physical quantity should not depend on the net topological charge, if the lattice volume is large enough. Even on a lattice with a fixed topological charge, local topological fluctuation could occur at different positions on the lattice keeping the net topological charge constant, and the frequency of the topological fluctuation is characterized by the topological susceptibility. In other words, the effect of fixing the net topology is a finite volume effect. (An important exception to this statement is the CP-odd quantities, such as the neutron electric dipole moment.) As we discussed in Sec. VI, hadron masses calculated at a fixed topology contains a finite volume correction of $O(1/V)$ to the physical value in the $\theta = 0$ vacuum [32]. Although the effect is quite large in the quenched QCD due to the sickness of quenched theory, we expect a small effect on dynamical lattices. Study of the topological charge dependence is underway as a part of our project of dynamical overlap fermion simulations.

ACKNOWLEDGMENTS

Numerical simulations are peformed on Hitachi SR11000 and IBM BlueGene/L at High Energy Accelerator Research Organization (KEK) under a support of its Large Scale Simulation Program No. 3 (FY2006). At an early stage, we also used NEC SX8 at Yukawa Institute for Theoretical Physics (YITP), Kyoto University. The authors thank YITP, where this work was initiated during the YITP workshop on "Actions and symmetries in lattice gauge theory" (YITP-W-05-25). H. F. and T. O. thank M. Lüscher for useful discussions. N. Y. thank T. Blum for discussions. This work is supported in part by the Grant-in-Aid of the Ministry of Education (No. 1315213, No. 16740147, No. 16740156, No. 17740171, No. 18340075, No. 18034011, and No. 18740167).

[1] D. B. Kaplan, Phys. Lett. B **288**, 342 (1992).
[2] Y. Shamir, Nucl. Phys. **B406**, 90 (1993).
[3] V. Furman and Y. Shamir, Nucl. Phys. **B439**, 54 (1995).
[4] H. Neuberger, Phys. Lett. B **427**, 353 (1998).
[5] H. Neuberger, Phys. Rev. D **61**, 085015 (2000).
[6] F. Berruto, R. Narayanan, and H. Neuberger, Phys. Lett. B **489**, 243 (2000).
[7] R. G. Edwards, U. M. Heller, and R. Narayanan, Nucl. Phys. **B535**, 403 (1998).
[8] M. Golterman and Y. Shamir, Phys. Rev. D **68**, 074501 (2003).
[9] M. Golterman, Y. Shamir, and B. Svetitsky, Phys. Rev. D **71**, 071502 (2005).
[10] M. Golterman, Y. Shamir, and B. Svetitsky, Phys. Rev. D **72**, 034501 (2005).
[11] S. Aoki, Phys. Rev. D **30**, 2653 (1984).
[12] For the domain-wall fermion the relevant operator is not H_W itself but a logarithm of the transfer matrix in the fifth dimension. They share the zero modes, and the near-zero modes of the both operators are closely related with each other.
[13] S. Aoki, T. Izubuchi, Y. Kuramashi, and Y. Taniguchi, Phys. Rev. D **62**, 094502 (2000).
[14] T. Blum *et al.*, Phys. Rev. D **69**, 074502 (2004).
[15] N. Christ (RBC and UKQCD Collaborations), Proc. Sci. LAT2005 (2006) 345.
[16] P. Hernandez, K. Jansen, and M. Lüscher, Nucl. Phys. **B552**, 363 (1999).
[17] P. M. Vranas, hep-lat/0001006.
[18] T. Izubuchi and C. Dawson (RBC Collaboration), Nucl. Phys. B, Proc. Suppl. **106**, 748 (2002).
[19] M. Lüscher (private communication).
[20] H. Fukaya, hep-lat/0603008.
[21] P. M. Vranas, Phys. Rev. D **74**, 034512 (2006).
[22] S. Duane, A. D. Kennedy, B. J. Pendleton, and D. Roweth, Phys. Lett. B **195**, 216 (1987).
[23] J. Gasser and H. Leutwyler, Phys. Lett. B **188**, 477 (1987).
[24] H. Fukaya, S. Hashimoto, T. Hirohashi, K. Ogawa, and T. Onogi, Phys. Rev. D **73**, 014503 (2006).
[25] W. Bietenholz, K. Jansen, K. I. Nagai, S. Necco, L. Scorzato, and S. Shcheredin, J. High Energy Phys. 03 (2006) 017.
[26] M. Lüscher, Nucl. Phys. **B549**, 295 (1999).
[27] Y. Iwasaki, Report No. UTHEP-118.
[28] M. Creutz, Phys. Rev. D **70**, 091501 (2004).
[29] Y. Namekawa *et al.* (*CP*-PACS Collaboration), Phys. Rev. D **70**, 074503 (2004).
[30] R. Gupta, G. W. Kilcup, and S. R. Sharpe, Phys. Rev. D **38**, 1278 (1988).
[31] L. Giusti, C. Hoelbling, M. Lüscher, and H. Wittig, Comput. Phys. Commun. **153**, 31 (2003).
[32] R. Brower, S. Chandrasekharan, J. W. Negele, and U. J. Wiese, Phys. Lett. B **560**, 64 (2003).
[33] D. Galletly *et al.*, hep-lat/0607024.
[34] A. Hasenfratz and T. A. DeGrand, Phys. Rev. D **49**, 466 (1994).
[35] W. J. Lee and D. Weingarten, Phys. Rev. D **59**, 094508 (1999).
[36] P. Weisz, Phys. Lett. B **100**, 331 (1981).
[37] H. Kawai, R. Nakayama, and K. Seo, Nucl. Phys. **B189**, 40 (1981).
[38] S. Sint and R. Sommer, Nucl. Phys. **B465**, 71 (1996).
[39] G. Bhanot, Phys. Lett. B **108**, 337 (1982).
[40] T. Blum *et al.*, Phys. Rev. D **50**, 3377 (1994).
[41] F. Farchioni *et al.*, Eur. Phys. J. C **39**, 421 (2005).
[42] S. Aoki *et al.* (JLQCD Collaboration), Phys. Rev. D **72**, 054510 (2005).
[43] Z. Fodor, S. D. Katz, and K. K. Szabo, J. High Energy Phys. 08 (2004) 003.
[44] T. A. DeGrand and S. Schaefer, Phys. Rev. D **71**, 034507 (2005).
[45] T. A. DeGrand and S. Schaefer, Phys. Rev. D **72**, 054503 (2005).
[46] N. Cundy, S. Krieg, G. Arnold, A. Frommer, T. Lippert, and K. Schilling, hep-lat/0502007.